UC Irvine
UC Irvine Previously Published Works

Title
Intracellular domain of the IFNaR2 interferon receptor subunit mediates transcription via Stat2

Permalink
https://escholarship.org/uc/item/37w103pg

Journal
Journal of Cellular Physiology, 204(2)

ISSN
0021-9541

Authors
El Fiky, Ashraf
Arch, Allison E
Krolewski, John J

Publication Date
2005-08-01

Peer reviewed

eScholarship.org Powered by the California Digital Library
University of California

Nuclear transit of the intracellular domain of the interferon receptor subunit IFNaR2 requires Stat2 and Irf9

Ashraf El Fiky [a, 1], Pete Pioli [a], Arif Azam [a], Kiwon Yoo [a],

Kent L. Nastiuk [a] and John J. Krolewski [a, b] *

[a] Department of Pathology and Laboratory Medicine

[b] Chao Family Comprehensive Cancer Center

School of Medicine

University of California, IRVINE

Irvine, CA 92679

*Corresponding author:
Phone: 949-824-4089
FAX: 949-824-2160
Email: jkrolews@uci.edu

Postal address: Department of Pathology and Laboratory Medicine
University of CA, IRVINE
Medical Sciences I, Room D450
Irvine, CA 92697-4800

Abbreviations: GFP, green fluorescent protein; IFN, interferon; ICD, intracellular domain; Irf9, Interferon regulatory factor 9; PS, presenilin; RIP, regulated intramembrane proteolysis; NLS, nuclear localization signal

[1]Present address:

Laboratory of Molecular Immunoregulation
National Cancer Institute
Frederick, MD 21702

Abstract

Regulated intramembrane proteolysis (RIP) is the primary signaling mechanism for some receptors, such as Notch and the amyloid precursor protein. In addition, some receptor type tyrosine kinases, such as HER4, are able to signal via both kinase activation and regulated receptor proteolysis. Previously, we showed that the IFNaR2 subunit of the type I interferon receptor can be cleaved in a two step process that resembles RIP and that the IFNaR2 intracellular domain (IFNaR2-ICD) can mediate gene transcription in a Stat2 dependent manner. Here, we demonstrate that IFNaR2-ICD, Stat2 and Irf9 form a ternary complex. Furthermore, Stat2 and Irf9 are required for the nuclear transit of a GFP-linked IFNaR2-ICD construct (GFP-ICD). Additional experiments monitoring the nuclear localization of GFP-ICD demonstrate that Stat2 serves an adaptor role, mediating the interaction between the IFNaR2-ICD and Irf9, while the bipartite nuclear localization signal within Irf9 is the primary determinant driving nuclear transit of the ICD containing complex. Overall, the data suggest that liberation of the IFNaR2-ICD by regulated proteolysis could trigger a novel mechanism for moving the transcription factor Stat2 to the nucleus.

Key words: interferon, receptor, IFNaR2, Stat2, Irf9, nuclear translocation, regulated proteolysis

1. Introduction

The type I interferons (IFNs) [1] are prototypical members of the family of helical cytokines [2]. These IFNs bind to a heteromeric receptor composed of two subunits, IFNaR1 and IFNaR2 [3, 4], which utilize the JAK tyrosine kinases, Jak1 and Tyk2, and STAT transcription factors, including Stat1 and Stat2, to modulate gene transcription [5]. IFN binding triggers receptor dimerization and activation of the receptor associated JAKs, which in turn phosphorylate a key tyrosine residue on IFNaR1, creating a docking site for Stat2 [6]. Stat2 and Stat1 are subsequently phosphorylated, and assemble into heterodimeric complexes via reciprocal SH2-phosphotyrosine interactions [7]. The STAT heterodimer associates with interferon regulatory factor 9 (Irf9) forming the ISGF3 complex, then translocates to the nucleus and binds to the interferon-stimulated gene response element, which is located upstream of a large number of IFN-regulated genes [8, 9].

In contrast to such tyrosine kinase driven signaling, regulated intramembrane proteolysis is a mechanistically simple and evolutionarily conserved mechanism for initiating signaling from a membrane protein localized either to the cell surface or an organelle membrane [10, 11]. The key biochemical event is the cleavage of a peptide bond within a transmembrane domain, with concomitant release of the extracellular and/or intracellular domains. One of the best characterized examples of RIP is signaling via the receptor Notch [12]. An initial, regulated cleavage within a juxtamembrane region of the extracellular domain, mediated by the metalloprotease TACE (also known as ADAM-17), releases the extracellular domain [13, 14]. The residual membrane-bound stub is further processed by the intramembrane proteases presenilin (PS) 1 and/or 2, which are part of a multi-protein complex known as γ-secretase [15]. This cleavage event releases the intracellular domain, which translocates to the nucleus and regulates gene transcription [16]. While Notch seems to signal exclusively via RIP, other receptors utilize RIP in conjunction with kinase signaling mechanisms. For example, signaling by HER4, a receptor protein tyrosine kinase that is sequentially processed by TACE and presenilins [17, 18], requires both proteolytic processing and intact kinase activity [19, 20].

We have recently found that phorbol ester and type I IFNs induce proteolytic cleavage of the IFNaR2 receptor subunit in a manner that resembles the two-step RIP cleavage of Notch [21]. Subsequently, we

demonstrated that the intracellular domain of IFNaR2 (IFNaR2-ICD) can mediate gene transcription in a Stat2 dependent manner [22]. In this report, we investigate additional aspects of the regulated proteolysis of this receptor, demonstrating that Stat2 and Irf9 can facilitate the translocation of the IFNaR2-ICD to the nucleus.

2. Material and methods

2.1. Cell culture

Human embryonic kidney HEK293T cells (H. Young, Columbia University, College of Physicians and Surgeons, USA) were grown in Dulbecco's modification of Eagle's media, plus 10% heat-inactivated fetal calf serum. Mutant cell lines (Stat2-deficient U6A cells [23] and Irf9-deficient U2A cells [24]) derived from a human fibrosarcoma cell line (HT1080) were obtained from G. Stark (Lerner Research Institute, USA) and grown in the same media.

2.2. Plasmid DNA constructs

Plasmids encoding glutathione-S-transferase (GST) fused to the IFNaR2-ICD (GST-ICD and GST-ICDm1, containing alanines in place of the acidic residues DEDD at codons 435-438; Fig. 1A) were described previously [25]. PfuI polymerase was used to amplify the wild type IFNaR2-ICD (or an m1 mutant with alanines at codons 435-438 in place of DEDD) which spans amino acids 265 to the carboxyl terminus. This DNA was digested with EcoRI and ligated into pEGFP (Clontech) to create plasmids encoding GFP-ICD and GFP-ICDm1 (Fig. 1A). To create a plasmid encoding Stat2-Δ235 lacking GFP (Fig. 1B), an EcoRI fragment from pGFP-Stat2-Δ235 (provided by N. Reich (Stony Brook University, USA) [26]) containing the open reading frame (ORF) of Stat2-Δ235 was cloned into the eukaryotic expression vector pMT2T (a new stop codon was derived from the vector sequence). A plasmid encoding an amino-terminally FLAG tagged Irf9 (pEF-FLAG-huIRF9) was prepared using PfuI polymerase to amplify the Irf9 ORF from pCMV-huIRF9 (from D. Levy, New York University School of Medicine, USA). This was cloned into the MluI site of the eukaryotic expression vector pEF, which contains an initiation codon and amino-terminal FLAG tag cassette (Fig. 1C). Similarly, plasmids encoding the two halves of Irf9 (Fig. 1C) were constructed by PCR and cloned into pEF to generate amino-terminally FLAG tagged versions. The plasmid pEF-FLAG-huIRF9-Cter encodes residues 199-393 of the full length Irf9; pEF-FLAG-huIRF9-Nter encodes residues 1-199. A plasmid encoding a GFP-Irf9 fusion construct (pEGFP-Irf9) was provided by C. Horvath (Evanston Northwestern Healthcare, USA) [27]. A plasmid (pEGFP-Irf9-5A) containing mutations in five residues of the bipartite NLS (KKKRR-66,68,70,83,85-AAAAA) was produced by two step, overlap PCR [28], which generated a PstI-HindIII fragment containing the mutations in residues 66, 68 and 70. This fragment was digested and cloned into a plasmid encoding a version of GFP-Irf9 with mutations at residues 83 and 85 (also from C. Horvath). The plasmid pEF-FLAG-huIRF9-5A (encoding a Flag-tagged Irf9 NLS mutant) was prepared by amplifying the Irf9 ORF from pEGFP-Irf9-5A as described above. All PCR-derived plasmid constructs were sequenced.

2.3. Affinity precipitation and immunoblotting

GST fusion proteins were prepared from bacteria expressing the fusion coding sequences under *lacZ* operator control. Cultures were grown to an A_{600} of 0.6, induced for 3 h by the addition of 100 mM isopropyl-beta-D-thiogalactopyranoside, pelleted, and lysed by the addition of lysozyme (100 μg/mL). The lysate was sonicated, insoluble protein and debris were pelleted and the supernatant was incubated with glutathione-agarose beads (Sigma) and washed with 100 mM NaCl, 10 mM Tris-HCl pH 8.0, 1 mM EDTA, 1% Triton X-100, 0.1% Sarkosyl to recover fusion proteins bound to beads. Next, affinity precipitation was performed by incubating the bead-bound fusion proteins with appropriate post-nuclear supernatants of lysates from HEK293T cells, transfected with the appropriate constructs, using calcium-phosphate precipitates [25, 29]. Two days post-transfection, cells were lysed in 1% NP40 and Tris-buffered saline (pH 8.0), as described previously [25]. After washing in 100 mM NaCl, 10 mM Tris-HCl pH 8.0, 1 mM EDTA, 1% NP40, bound protein complexes were eluted in sample buffer, electrophoresed on SDS-polyacrylamide gels, immunoblotted to nitrocellulose, blocked in 5% non-fat dry milk dissolved in TBS plus 0.2% Tween-20 and probed overnight at room temperature with antibodies. The primary antibodies were either a rabbit anti-human Stat2 antibody (from C. Schindler, Columbia University, USA) directed against amino acids 661-806 (used at 1:25,000 dilution) or a rabbit anti-FLAG antibody (F7425, Sigma; used at 1:5,000 dilution). Filters were washed, incubated with goat anti-rabbit horseradish peroxidase linked secondary antibody (Pierce) for 2-4 h at room temperature, washed and finally incubated with chemiluminescence reagent (Super Signal West Pico; Pierce) and then exposed to film (Fig. 2A) or a cooled charged-coupled digital camera (Kodak 4000R) (Fig. 2B).

2.4. Fluorescence microscopy

U6A cells (1.2 x 10^3 cells seeded into 24-well cluster dishes the night before) were transfected with 0.5 μg of GFP-ICD plasmid and 1 μg of additional plasmids as appropriate in individual experiments, using 2 μL of Lipofectamine and 3 μL of PLUS reagent (Invitrogen), following the manufacturer's directions. In some cases, U6A cells were transfected with similar volumes of Lipofectamine-2000. After 1 d, cells were trypsinized and re-seeded on 22 mm glass coverslips in 3.5-cm dishes. U2A cells (seeded as per U6A cells) were transfected with 2.5 μg of appropriate GFP-ICD encoding plasmid, 2.5 μg of appropriate Stat2 expressing plasmid and/or 0.5 μg of an Irf9

expressing plasmid, using a calcium-phosphate transfection protocol [25, 29]. Five hours post-transfection, cells were subjected to glycerol shock (20% glycerol in 150 mM NaCl, 10 mM Tris-HCl pH 7.4), trypsinized and re-seeded on coverslips in 3.5 cm dishes. HEK293T cells were transfected essentially as described for U2A cells, except that 8.0 x 10^5 cells were seeded the night before into 6-cm dishes, 10 µg of plasmid DNA was used and coverslips were coated with fibronectin (10 µg/mL diluted into media) prior to cell attachment. One or two days following transfection, cells adherent to the coverslips were fixed with 4% (w/v) paraformaldehyde in phosphate-buffered saline, counterstained with Hoechst 332581 and visualized under a Nikon Eclipse E600 fluorescent microscope. Images were captured with a Spot RT digital camera and accompanying software (Spot v3.5.9). All cells were photographed under identical exposure time and gain settings. Photos were coded and blinded observers scored fluorescence intensity by eye, using a scale of 0, 1 and 2, corresponding to no fluorescence, weak fluorescence and strong fluorescence. Images are representative of reproducible results selected from 2-5 independent experiments.

2.5. Statistical analysis

Confidence intervals for the nuclear fluorescence data scored at 2 in Figs. 3-6 were computed via the modified Wald method using the Graphpad™ website calculator at: http://www.graphpad.com/-quickcalcs/index.cfm (see Supplementary data). The non-parametric Mann-Whitney U-test was used to calculate p values for the entire set of nuclear fluorescence data in Figs. 3-6 employing the web-based software provided by R. Lowry (Vasser College, USA) at http://faculty.vassar.edu/lowry/utest.html (see Supplementary data).

3. Results

3.1 The IFNaR2-ICD forms a complex with Stat2 and Irf9

Previously, we demonstrated that the IFNaR2 intracellular domain can translocate to the nucleus [21], suggesting that the ICD either contains an inherent NLS or binds to other proteins that facilitate nuclear translocation. In addition, we confirmed earlier reports [30-32] that the intracellular portion of IFNaR2 binds Stat2 in a constitutive, ligand-independent manner [25, 33]. Since Irf9 is known to bind Stat2 [34, 35], we hypothesized that Stat2 recruits Irf9 into a complex with the IFNaR2-ICD. Irf9, which contains a DNA binding domain (DBD) [36] and a nuclear localization signal (NLS) [26, 27], might in turn provide one or both of these functions to a tri-molecular complex consisting of the IFNaR2-ICD, Stat2 and Irf9. To determine if Stat2 can serve as an adaptor physically linking the IFNaR2-ICD to Irf9, an affinity precipitation protocol was employed. Bacterial GST proteins, fused to the wild type IFNaR2 intracellular domain (GST-ICD) or a mutant version (GST-ICDm1), were partially purified on agarose-glutathione beads. In the ICDm1 mutation, four acidic residues (DEDD) have been converted to alanines (Fig. 1A), generating a version of the IFNaR2-ICD which binds Stat2 weakly [25]. HEK293T cells were transfected with either Stat2 or FLAG-tagged Irf9, separately or in combination, and the resulting lysates were incubated with the bead-bound GST fusion proteins. The complexes were eluted from the beads and immunoblotted with the indicated antibodies (Fig. 2A). The GST-ICD fusion bound Irf9 only in cells over-expressing Stat2 (compare lanes 1 and 2), indicating that Irf9 binds the IFNaR2-ICD via Stat2. The affinity precipitation of Stat2 and, therefore, Irf9 was greatly reduced when the GST-ICDm1 fusion was employed (compare lanes 1 and 4), supporting the idea that the IFNaR2-ICD binds Irf9 via Stat2.

3.2. The carboxyl terminus of Irf9 is required for Stat2 dependent binding to the IFNaR2-ICD

The carboxyl terminal 193 amino acids of Irf9 bind Stat2 in the context of the ISGF3 complex which forms following type I interferon (IFN) binding to its cognate receptors [34]. To confirm that this same domain mediates Stat2 binding in the context of the IFNaR2-ICD complex, we constructed amino- and carboxyl-terminal truncated versions of Irf9 (N-Irf9 and C-Irf9, respectively; see Fig. 1C). The GST-ICD fusion affinity precipitated Stat2 equally in each case (Fig. 2B, upper panels; Stat2 corresponds to the slower migrating band). However, only the C-Irf9 protein was affinity precipitated from the same lysates (Fig. 2B, middle panels). Thus, Irf9 binds Stat2 when it is part of an IFNaR2-ICD complex in the same manner that it

binds the Stat2-Stat1 dimer within the ISGF3 complex.

3.3. Stat2 is required for IFNaR2-ICD nuclear import

One possible mechanism for IFNaR2-ICD movement to the nucleus is via the NLS of Irf9. Since Stat2 tethers Irf9 to the IFNaR2-ICD (Fig. 2), then Stat2 might be required for nuclear transit of the complex. To test this possibility, we employed a construct in which GFP is fused to the IFNaR2-ICD, and a cell line (U6A) deficient in the expression of Stat2. Previously, we have shown that following transient transfection, GFP-ICD localized to the nucleus of U2OS cells [21]. In contrast, in U6A cells, GFP-ICD was predominantly cytoplasmic (Fig. 3, transfection I). Complementation with wild type Stat2 shifted the GFP-ICD protein into the nucleus (Fig. 3, transfection II). As a control, we also examined the sub-cellular localization of the GFP-ICD fusion carrying the m1 mutation that substantially disrupts Stat2 binding. This construct failed to translocate to the nucleus even when cells were complemented with wild type Stat2 (Fig. 3, transfections III-IV), suggesting that Stat2 must be present and bound to the IFNaR2-ICD to facilitate the accumulation of the IFNaR2-ICD in the nucleus. Two statistical comparisons support these observations. First, focusing on the percentage of nuclei displaying strong GFP fluorescence (scored 2 in Fig. 3), there is an increase from <15% among all of the control transfections (I, III and IV) to ~50% in the cells transfected with wild type Stat2 (II), with no overlap in the 95% confidence interval (CI) between II and I, III or IV (see Supplementary data, Table S1). Second, pair-wise application of the Mann-Whitney U-test (see Materials and methods) to the aggregate data from each transfection reveals that the nuclear fluorescence in transfection II differs from that in transfections I, III or IV ($p < 0.01$; Table S1).

3.4 Irf9 is also required for IFNaR2-ICD nuclear import

Since Irf9 forms a tri-molecular complex with IFNaR2-ICD and Stat2 (Fig. 2) and contains an NLS [26, 27], we examined the role of Irf9 in the nuclear import of the IFNaR2-ICD. The experimental approach was identical to that used in Fig. 3, again employing Stat2-deficient U6A cells and complementing the cells with either wild type Stat2 or a Stat2-Δ235 construct that does not bind Irf9 [26]. Similar to full length Stat2, Stat2-Δ235 bound the IFNaR2-ICD (data not shown). If Irf9 must bind Stat2 to facilitate nuclear translocation of the IFNaR2-ICD, then when U6A cells are transfected with GFP-ICD and Stat2-Δ235, the GFP-ICD should remain predominantly in the cytoplasm. Fig. 4 shows that, as predicted, the Stat2-Δ235 construct is ineffective in moving the GFP-ICD protein to the nucleus (compare transfections I and III). However, complementation with wild type Stat2 produced an increase in IFNaR2-ICD nuclear localization (Fig. 4, transfection II), very similar to the results shown in Fig. 3, transfection II. The difference in the intensity of nuclear fluorescence of cells shown in transfections II and III in Fig. 4 is significant, based on the same two statistical criteria used in Fig. 3 (see Supplementary data, Table S2).

To confirm the role of Irf9 in the nuclear import of the IFNaR2-ICD, we again monitored the sub-cellular localization of the GFP-ICD construct, this time employing Irf9-deficient U2A cells in place of Stat2-deficient U6A cells. The GFP-ICD was predominantly cytoplasmic in U2A cells (Fig. 5A, transfection I), suggesting that Irf9 was indeed required for the nuclear translocation of the IFNaR2-ICD. When the GFP-ICD transfected U2A cells were complemented with wild type Irf9 (Fig. 5A, transfection II), the level of nuclear fluorescence was not significantly increased, indicating that the IFNaR2-ICD remained predominantly cytoplasmic. Assuming that Stat2 acts as a bridge to link the IFNaR2-ICD to Irf9, one possible explanation for this latter observation is that the

endogenous level of Stat2 in the U2A cells was insufficient to perform the bridging function on the over-expressed proteins in the experiment. Specifically, we hypothesized that there was not enough endogenous Stat2 to allow for the formation, and subsequent translocation, of a detectable number of GFP-ICD-Stat2-Irf9 ternary complexes into the nuclei of the transfected cells. Indeed, correcting this possible 'imbalance' by also over-expressing wild type Stat2 markedly increased the level of nuclear GFP-ICD (Fig. 5A, compare transfections II and III). In contrast, co-expression of the Stat2-Δ235 construct with Irf9 was unable to induce nuclear accumulation of the GFP-ICD (Fig. 5A, transfection IV), confirming the adaptor function of Stat2 in the process of nuclear translocation. The increase in nuclear fluorescence for transfection III was statistically significant relative to the control transfections (see Supplementary data, Table S3). A control experiment was also performed to demonstrate that, in Irf9 deficient U2A cells, over-expression of wild type Stat2 alone did not alter the nuclear localization of the GFP-ICD (Fig. 5B and Supplementary data, Table S4).

3.5 The Irf9 NLS is required for IFNaR2-ICD nuclear import

Lau *et al.* [27] previously identified a bi-partite NLS located within the DBD of Irf9. They employed a GST-Irf9 fusion protein to show that mutations in either half of the bi-partite NLS reduced the nuclear localization of Irf9. To test the physiological relevance of the Irf9 NLS, we substituted five alanines for basic residues in both halves of the NLS (Irf9-5A; see Fig. 1C and Materials and methods) and transfected this construct into 293T cells. Consistent with the observations of Lau et al. [27] this mutant form of Irf9 demonstrated a decrease in nuclear localization and a corresponding increase in cytoplasmic fluorescence (Supplementary data, Fig. S1). To evaluate the role of the Irf9 NLS in IFNaR2-ICD nuclear translocation, we performed an experiment similar to that in Fig. 5A, introducing GFP-ICD, Stat2 and Irf9 or Irf9-5A into Irf9-deficient U2A cells, and scoring for nuclear fluorescence. Mutation of the Irf9 NLS significantly inhibited nuclear localization of the GFP-ICD (Fig. 6, compare transfection II with transfections I and III, also see Supplemental data, Table S5), consistent with our hypothesis that the Irf9 NLS directs the IFNaR2-ICD to the nucleus.

4. Discussion

Multiple lines of biochemical and genetic evidence support a role for canonical JAK-STAT signaling downstream from the type I interferon receptor [2, 5, 8]. However, as in the case of HER4, tyrosine kinase and STAT driven signaling can function coordinately with RIP signaling [19, 20]. While investigating the canonical JAK-STAT pathway for IFN signaling [25, 33], we demonstrated that i) Stat2 can bind IFNaR2 constitutively; ii) this binding is stronger than the binding of phosphorylated-IFNaR1 to Stat2 that occurs following IFN-driven receptor dimerization; and iii) the IFNaR2-Stat2 interaction is not required for canonical JAK-STAT signaling/gene regulation. These findings suggested that IFNaR2 might signal by other, non-canonical mechanisms and, indeed, we subsequently found that this subunit of the IFN receptor is proteolytically cleaved in a regulated manner that resembles signaling by other RIP substrates [21]. We also showed that the receptor ICD can modulate transcription via the TAD of the bound Stat2 molecule [22]. Moreover, we have recently demonstrated that IFNaR2 is a substrate for TACE (unpublished data, A. Saleh, P.P. and J.J.K.), which cleaves IFNaR2 in the extracellular domain, generating a transmembrane anchored 'stub' containing a short residual extracellular domain. It is believed that once such TACE cleavage has occurred, the stub is then constitutively processed by an intramembrane protease to liberate the ICD from the membrane [37].

A diverse group of >36 membrane proteins have been identified as substrates of the γ-secretase intramembrane protease

complex [37]. It has been suggested that RIP may have initially evolved as a mechanism for degrading residual fragments of membrane anchored proteins, but it is now abundantly clear that the liberated ICDs are functional [37]. In particular, at least 16 γ-secretase generated ICDs have been localized to the nucleus and at least 10 modulate transcription [38], including well characterized examples such as HER4 [17, 39, 40] and Notch [41]. Some RIP substrates, such as SREBP-2 and ErbB4, contain an NLS within the ICD, that mediates nuclear transit following cleavage. In the case of HER4, a classical arginine-rich NLS has been identified [39], while a non-standard NLS that binds ß-importin has been identified in SREBP2 [42]. These NLS motifs are non-functional when the ICD is tethered to the cell surface as part of the intact receptor, but direct nuclear transit of the ICD following intramembrane cleavage. For those receptors lacking an NLS in the ICD, associating proteins might provide such a signal.

In attempting to identify a mechanism for moving the IFNaR2 ICD to the nucleus, we noted that the IFNaR2 ICD binds constitutively to Stat2 [25] which in turn binds Irf9 [34, 35]. Stat2 contains a conditional NLS which is only active when Stat2 dimerizes with Stat1 and forms the ISGF3 complex [43, 44]. Since the ICD can transit to the nucleus in a ligand independent fashion [21], under conditions where little or no STAT dimerization occurs, it seems unlikely that Stat2 is directly providing an NLS for the ICD. Unphosphorylated Stat2 can also move to the nucleus due to its association with Irf9, which contains an arginine-lysine rich bipartite NLS (Fig. 1C) [27]. However, Stat2 possesses a strong nuclear export signal that over-rides the Irf9 NLS when these two proteins are assembled in a binary complex. Thus, while Stat2 (and Irf9) shuttle between the nucleus and cytoplasm, these two proteins reside predominately in the cytoplasm in the absence of IFN [26]. In this report, we sought to test the idea that when the IFNaR2 ICD is present in the cytoplasm, it forms a ternary complex with Irf9 and Stat2. Under these conditions Irf9, bound to the IFNaR2 ICD indirectly via Stat2, promotes the movement of this tri-molecular complex to the nucleus. This would represent a novel mechanism for delivering Stat2 to the nucleus.

First, we used an in vitro binding assay to show that Stat2, Irf9 and the IFNaR2 ICD form a tri-molecular complex (Fig. 2A). A GST-ICD fusion protein was able to affinity precipitate Irf9 only from cells expressing Stat2, consistent with Stat2 functioning as an adaptor between IFNaR2-ICD and Irf9. This is further supported by the observation that a mutant version of IFNaR2 (IFNaR2-ICDm1; Fig. 1B) previously shown to bind weakly to Stat2, was significantly less avid in binding Irf9 (Fig. 2A). Others have also demonstrated the formation of a complex containing Irf9 and Stat2 bound to the intracellular portion of IFNaR2 [45]. In this latter case, Irf9 binds IFNaR2 directly, not via Stat2, and the interaction is dependent on receptor lysine acetylation. Moreover, this is likely to be a distinct complex from the one we have characterized, as it is formed with the intact receptor and appears to play a role in canonical signaling.

Next, we employed a GFP-ICD fusion construct as a surrogate to study the movement of the IFNaR2-ICD-Stat2-Irf9 complex inside cells. Previously, we have shown that GFP-ICD is predominately nuclear in cells expressing the wild type Stat2 and Irf9 proteins [21]. In Stat2 deficient U6A cells, GFP-ICD was predominantly cytoplasmic, but mobilized to the nucleus when these cells are complemented with wild type Stat2 (Fig. 3). A version of GFP-ICD which binds Stat2 weakly (GFP-ICDm1) [25] was predominantly cytoplasmic even when U6A cells were complemented with Stat2, demonstrating that binding to Stat2 is required. These findings are, like those of the affinity precipitation studies in Fig. 2, consistent with the hypothesis that Stat2 is an adaptor. Taken together, the data point to a critical role of Stat2 in the tri-molecular

complex and demonstrate that strong binding of Stat2 to the IFNaR2-ICD is required for nuclear transit of the IFNaR2-ICD.

To explore the role of Irf9, we first demonstrated that the carboxyl-terminus of Irf9 was sufficient to form the IFNaR2-ICD-Stat2 complex (Fig. 2B). This is consistent with a prior report that Stat2 binds to Irf9 in this region [34] and supports our hypothesis that Irf9 binds the ICD via Stat2. Three sets of experiments, each monitoring the sub-cellular localization of the fluorescence of GFP-ICD, demonstrated a functional role for Irf9 in the nuclear transit of the ICD. In the first case (Fig. 4), the GFP-ICD was mainly nuclear when Stat2-deficient cells were complemented with wild type Stat2, but mostly nuclear when we employed a Stat2 deletion construct (Stat2-Δ235) lacking the carboxyl terminal 235 amino acids responsible for Irf9 binding. In the second set, GFP-ICD did not translocate to the nucleus in absence of Irf9, consistent with our hypothesis that Irf9 is required for IFNaR2-ICD nuclear transit (Fig. 5). Surprisingly, the GFP-ICD construct remained predominantly cytoplasmic when Irf9-deficient (U2A) cells were complemented with Irf9 (Fig. 5A). If Stat2 links the ICD to Irf9, then one possibility is that relatively low endogenous levels of Stat2 are not sufficient to translocate a detectable number of GFP-ICD molecules to the nucleus. Indeed, co-expression of Stat2 resulted in significant nuclear mobilization of the ICD. Control experiments (Fig. 5B) showed that GFP-ICD nuclear transit is not simply an artifact of Stat2 expression in the absence of Irf9. Finally, a third set of experiments (Fig. 6) demonstrated that the Irf9 NLS was critical for the nuclear translocation of the ICD. Specifically, mutating five key residues within the bi-partite NLS of Irf9 prevented nuclear localization.

5. Conclusions

The data in this report, along with previously published data, allow us to begin to formulate a model for RIP signaling via IFNaR2. We propose that the initial step is TACE activation via PKC-δ, a probable TACE activator [46] which can be triggered by type I IFNs [47]. PKC-δ activation is likely a result of JAK kinase activation. TACE cleaves IFNaR2 near the TMD, shedding the ectodomain and generating a transmembrane stub (unpublished data, A. Saleh, P.P. and J.J.K.). The stub is subsequently cleaved in a constitutive manner by the γ-secretase protease complex, containing PS1 and PS2 [21]. We now propose that this intramembrane cleavage event liberates the IFNaR2-ICD from the membrane as a complex with Stat2 and Irf9, with Stat2 tethering Irf9 to the ICD. Irf9 then provides a nuclear localization signal to move the ICD to the nucleus. We have previously shown that ICD-bound Stat2 can modulate transcription via its TAD [22]. While it remains to be determined if the ICD complex does indeed regulate physiological gene expression and whether regulated proteolysis mediates the IFN response, this report further supports the possibility of RIP signaling via an IFN receptor.

Acknowledgements

This work was supported by National Institute of Health grant CA056862 (to JJK). We wish to thank KimAnh Nguyen and Ryan Fuh for assistance in the construction of the Irf9 NLS mutant. We also wish to thank G. Stark, C. Schindler, D. Levy. N. Reich and C. Horvath for reagents as indicated in the Materials and methods.

References

[1] S. Pestka, J. Biol. Chem. 282 (2007) 20047-20051.
[2] J.L. Boulay, J.J. O'Shea, W.E. Paul, Immunity 19 (2003) 159-163.
[3] G. Uzé, G. Schreiber, J. Piehler, S. Pellegrini, Curr. Top. Microbiol. Immunol. 316 (2007) 71-95.
[4] N.A. de Weerd, S.A. Samarajiwa, P.J. Hertzog, J. Biol. Chem. 282 (2007) 20053-20057.
[5] D.E. Levy, J.E. Darnell, Nat. Rev. Mol. Cell Biol. 3 (2002) 651-662.
[6] H. Yan, K. Krishnan, A.C. Greenlund, S. Gupta, J.T.E. Lim, R.D. Schreiber, C. Schindler, J.J. Krolewski, EMBO J. 15 (1996) 1064-1074.

[7] K. Shuai, C.M. Horvath, L.H.T. Huang, S.A. Qureshi, D. Cowburn, J.E. Darnell, Cell 76 (1994) 821-828.
[8] J.E. Darnell, Science 277 (1997) 1630-1635.
[9] C. Schindler, D.E. Levy, T. Decker, J. Biol. Chem. 282 (2007) 20059-20063.
[10] A.J. Brown, L. Sun, J.D. Feramisco, M.S. Brown, J.L. Goldstein, Mol. Cell 10 (2002) 237-245.
[11] S. Urban, M. Freeman, Curr. Opin. Genet. Dev. 12 (2002) 512.
[12] D. Selkoe, R. Kopan, Annu. Rev. Neurosci. 26 (2003) 565-597.
[13] C. Brou, F. Logeat, N. Gupta, C. Bessia, O. LeBail, J.R. Doedens, A. Cumano, P. Roux, R.A. Black, A. Israel, Mol. Cell 5 (2000) 207-216.
[14] S. Jarriault, I. Greenwald, Dev. Biol. 287 (2005) 1-10.
[15] M.S. Wolfe, Biochemistry 45 (2006) 7931-7939.
[16] D. Barrick, R. Kopan, Cell 124 (2006) 883-885.
[17] C.Y. Ni, M.P. Murphy, T.E. Golde, G. Carpenter, Science 294 (2001) 2179-2181.
[18] C. Rio, J.D. Buxbaum, J.J. Peschon, G. Corfas, J. Biol. Chem. 275 (2000) 10379-10387.
[19] G.A. Vidal, A. Naresh, L. Marrero, F.E. Jones, J. Biol. Chem. 280 (2005) 19777-19783.
[20] S.P. Sardi, J. Murtie, S. Koirala, B.A. Patten, G. Corfas, Cell 127 (2006) 185-197.
[21] A.Z.M. Saleh, A.E. Arch, D. Neupane, J.J. Krolewski, Oncogene 23 (2004) 7076-7086.
[22] A. El Fiky, A.E. Arch, J.J. Krolewski, J. Cell. Physiol. 204 (2005) 567-573.
[23] S. Leung, S.A. Qureshi, I.M. Kerr, J.E. Darnell, G.R. Stark, Mol. Cell. Biol. 15 (1995) 1312-1317.
[24] X. Li, S. Leung, S. Qureshi, J.E. Darnell, G.R. Stark, J. Biol. Chem. 271 (1996) 5790-5794.
[25] V.-P. Nguyen, A.Z.M. Saleh, A.E. Arch, H. Yan, F. Piazza, J. Kim, J.J. Krolewski, J. Biol. Chem. 277 (2002) 9713-9721.
[26] G. Banninger, N.C. Reich, J. Biol. Chem. 279 (2004) 39199-39206.
[27] J.F. Lau, J.P. Parisien, C.M. Horvath, Proc. Natl. Acad. Sci. U S A 97 (2000) 7278-7283.
[28] S.N. Ho, H.D. Hunt, R.M. Horton, J.K. Pullen, L.R. Pease, Gene 77 (1989) 51-59.
[29] M. Jordan, F. Wurm, Methods 33 (2004) 136-143.
[30] S. Leung, X. Li, G.R. Stark, Science 273 (1996) 750-751.
[31] X. Li, S. Leung, I.M. Kerr, G.R. Stark, Mol. Cell. Biol. 17 (1997) 2048-2056.
[32] O.W. Nadeau, P. Domanski, A. Usacheva, S. Uddin, L.C. Platanias, P. Pitha, R. Raz, D. Levy, B. Majchrzak, E. Fish, O.R. Colamonici, J. Biol. Chem. 274 (1999) 4045-4052.
[33] A.Z. Saleh, V.P. Nguyen, J.J. Krolewski, Biochemistry 41 (2002) 11261-11268.
[34] C.M. Horvath, G.R. Stark, I.M. Kerr, J.E. Darnell, Jr., Mol. Cell. Biol. 16 (1996) 6957-6964.
[35] M. Martinez-Moczygemba, M.J. Gutch, D.L. French, N.C. Reich, J. Biol. Chem. 272 (1997) 20070-20076.
[36] D.S. Kessler, S.A. Veals, X.-Y. Fu, D.E. Levy, Genes & Develop. 4 (1990) 1753-1765.
[37] D.J. Selkoe, M.S. Wolfe, Cell 131 (2007) 215-221.
[38] A.L. Parks, D. Curtis, Trends Genet. 23 (2007) 140-150.
[39] C.C. Williams, J.G. Allison, G.A. Vidal, M.E. Burow, B.S. Beckman, L. Marrero, F.E. Jones, J. Cell Biol. 167 (2004) 469-478.
[40] Y. Zhu, L.L. Sullivan, S.S. Nair, C.C. Williams, A.K. Pandey, L. Marrero, R.K. Vadlamudi, F.E. Jones, Cancer Res. 66 (2006) 7991-7998.
[41] O.Y. Lubman, S.K. Korolev, R. Kopan, Mol. Cell 13 (2004) 619-626.
[42] E. Nagoshi, N. Imamoto, R. Sato, Y. Yoneda, Mol. Biol. Cell 10 (1999) 2221-2233.
[43] L.J. Medeiros, S.C. Peiper, L. Elwood, T. Yano, M. Raffeld, E.S. Jaffe, Hum. Pathol. 22 (1991) 1150-1157.
[44] R. Fagerlund, K. Melen, L. Kinnunen, I. Julkunen, J. Biol. Chem. 277 (2002) 30072-30078.
[45] X. Tang, J.S. Gao, Y.J. Guan, K.E. McLane, Z.L. Yuan, B. Ramratnam, Y.E. Chin, Cell 131 (2007) 93-105.
[46] J.R. Doedens, R.A. Black, J. Biol. Chem. 275 (2000) 14598-14607.
[47] S. Uddin, A. Sassano, D.K. Deb, A. Verma, B. Majchrzak, A. Rahman, A.B. Malik, E.N. Fish, L.C. Platanias, J. Biol. Chem. 277 (2002) 14408-14416.

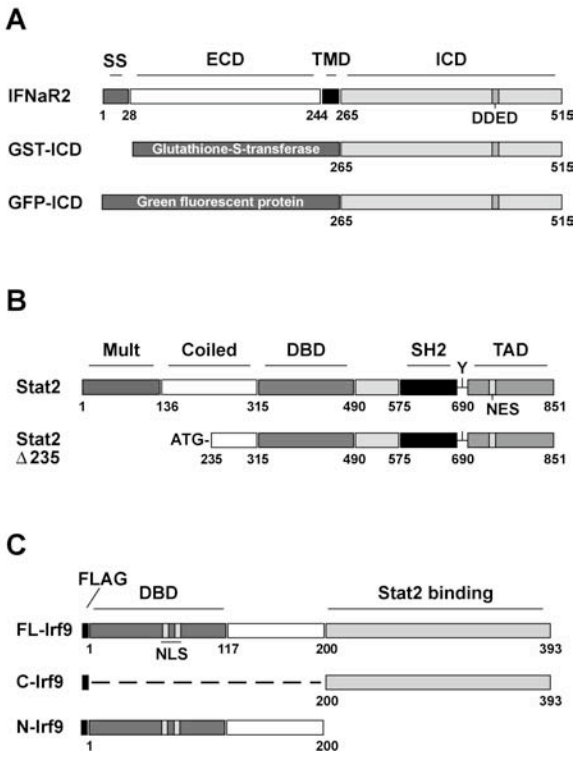

Fig. 1. Schematic diagrams of protein constructs. A, IFNaR2 constructs. Full length IFNaR2, including the signal sequence (SS), extracellular domain (ECD), transmembrane domain (TMD) and intracellular domain (IFNaR2-ICD) is shown on the top. Numbers correspond to the coding sequence of the human IFNaR2c open reading frame. In the m1 mutant, the acidic amino acids at positions 435 to 438 (DDED) are mutated to alanines. The second line shows GST-ICD, a fusion construct joining the IFNaR2-ICD to GST. Similarly, the third line depicts a fusion with EGFP. B, Stat2 constructs. The top line shows wild type Stat2 including the amino terminal multimerization domain (Mult), the coiled-coil domain (Coiled), DNA binding domain (DBD), an unlabeled linker domain, the src-homolgy-2 (SH2) domain, the tyrosine 690 phosphorylation site, a nuclear export signal (NES; residues 740-751) and the carboxyl-terminal transactivation domain (TAD). The second line diagrams a derivative lacking the multimerization domain and part of the coiled-coil domain which together comprise the amino-terminal 235 amino acids responsible for binding to Irf9 (Stat2Δ235). An ATG and Kozak translation initiation sequence have been fused directly to residue 236. C, Irf9 constructs. The top line is a schematic of an amino-terminal FLAG-tagged Irf9 construct depicting the DBD, a bipartite NLS spanning amino acids 66-85 and the carboxyl-terminal domain responsible for binding to Stat2. The second line shows C-Irf9, corresponding to the carboxyl terminal half of the protein, while the third line depicts N-Irf9, corresponding to the amino terminal half.

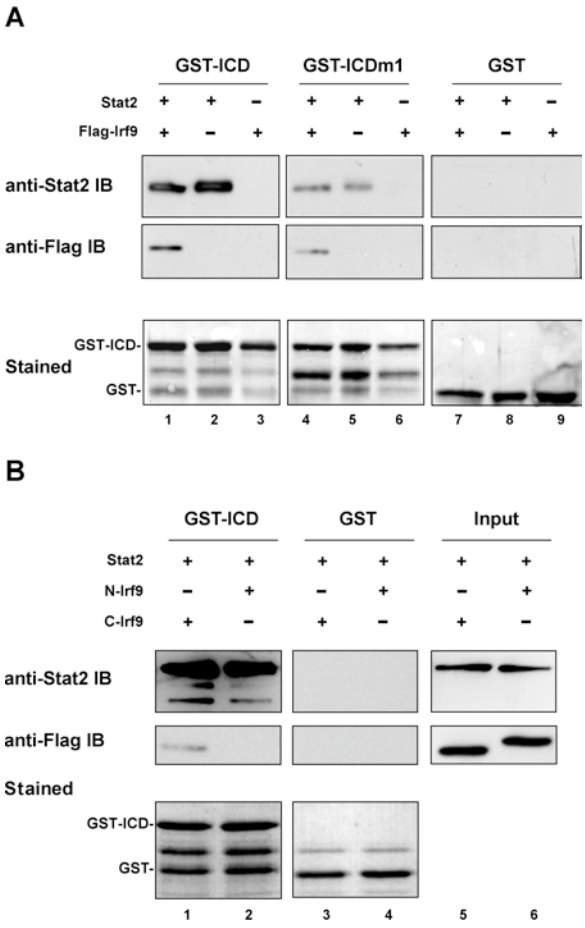

Fig. 2. The IFNaR2-ICD binds Irf9 via Stat2. A, Stat2 is required for IFNaR2-ICD binding to Irf9. HEK293T cells were transfected with plasmids encoding Stat2 and/or FLAG-tagged Irf9, as indicated. Lysates were incubated with glutathione-agarose beads bound to GST-ICD (lanes 1-3), GST-ICDm1 (lanes 4-6) or GST (lanes 7-9) and the protein complexes were immunoblotted. The filter was stained, cut in two and the lower molecular weight proteins (<80 kD) were incubated with anti-FLAG antibody, while the higher molecular weight proteins were incubated with anti-Stat2 antibody, as indicated. Part of the Ponceau red stained filter (Stained) is shown to demonstrate GST protein recovery. The lower molecular weight bands in lanes 1-6 are GST degradation products. B, the carboxyl-terminal domain of Irf9 is required for Stat2 binding to IFNaR2-ICD. HEK293T cells were transfected and processed as in A, with plasmids encoding the indicated constructs (see Fig. 1C). In the anti-Stat2 immunoblot, Stat2 is the upper band. Lanes 5 and 6 show the input lysates representing ~2% of the material used in the affinity precipitations.

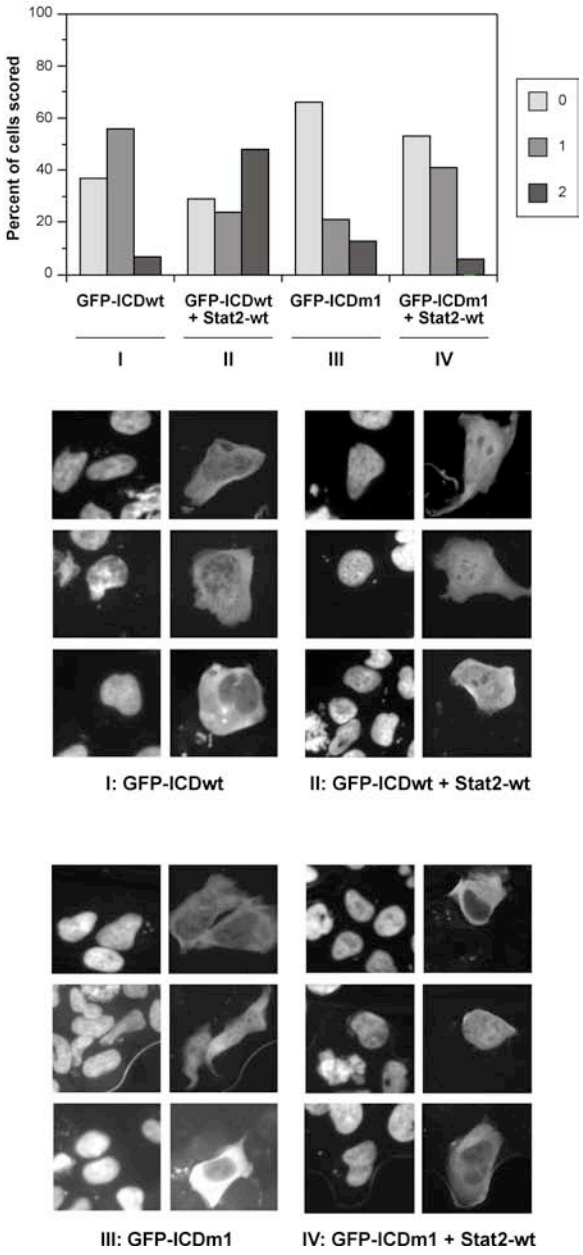

Fig 3. Stat2 is required for nuclear localization of GFP-ICD. Stat2-deficient U6A cells were transiently transfected with plasmids encoding wild type (wt) or mutant (m1) forms of the IFNaR2-ICD fused to GFP (GFP-ICD) plus either vector or wild type Stat2-encoding (Stat2-wt) plasmids, as indicated. Cells were fixed, stained with a nuclear dye, visualized under a fluorescent microscope and the percentage of nuclei at each level of green fluorescence intensity was scored as described in the Materials and methods, and plotted at the top. Cells displaying the highest level of fluorescence were scored 2. Statistical analysis of the plotted data is shown in the Supplement (Table S1). Representative cells from each transfected culture are shown in the bottom part of the figure. In each pair of columns, images on the left correspond to blue fluorescence due to nuclear staining, while those on the right correspond to green fluorescence due to GFP.

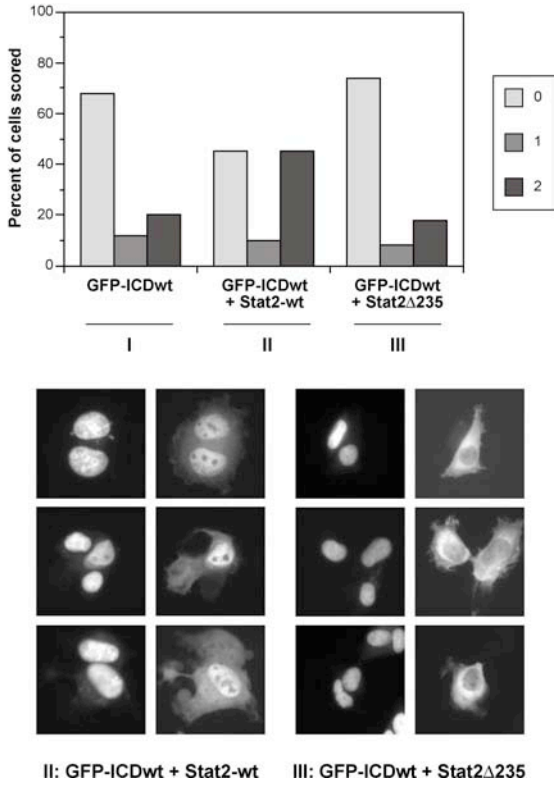

Fig. 4. Stat2 must interact with Irf9 to facilitate nuclear localization of GFP-ICD. Stat2-deficient U6A cells were transiently transfected with plasmids encoding IFNaR2-ICD fused to GFP (GFP-ICDwt) plus plasmids encoding either vector, wild type Stat2 or Stat2Δ235, as indicated. Similar to Fig. 3, cells were processed, visualized and scored; statistical analysis of the plotted data is shown in the Supplement (Table S2) and representative cells from two of the transfected cultures are shown in the bottom part of the figure.

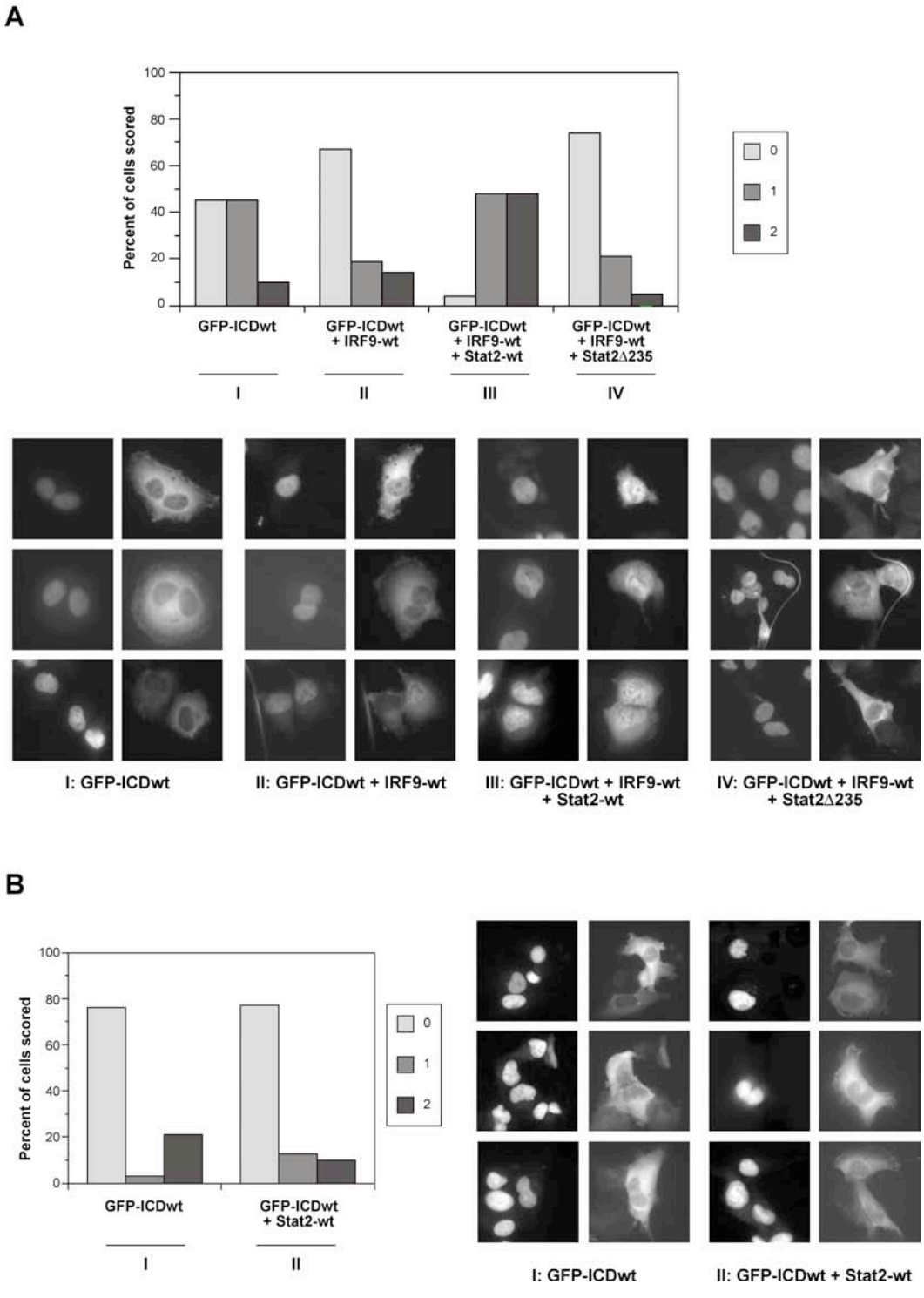

Fig. 5. Irf9 is required for nuclear localization of GFP-ICD. A, GFP-ICD localizes to the nucleus of Irf9-deficient cells transfected with Irf9 and Stat2. Irf9-deficient U2A cells were transiently transfected with plasmids encoding IFNaR2-ICD fused to GFP (GFP-ICDwt) plus plasmids encoding either Irf9 (Irf9-wt), wild type Stat2 or Stat2D235, as indicated. B, Stat2 over-expression alone does not lead to nuclear translocation of the IFNaR2-ICD. Similar to A, except that cells were transfected with either GFP-ICD alone or in combination with wild type Stat2. In both A and B, vector DNA was used to equalize the amount of DNA in each transfection. Similar to Fig. 3, cells were processed, visualized and scored; statistical analysis of the plotted data is shown in the Supplement (Table S3-S4) and representative cells from each transfected culture are shown in the bottom part of the figure.

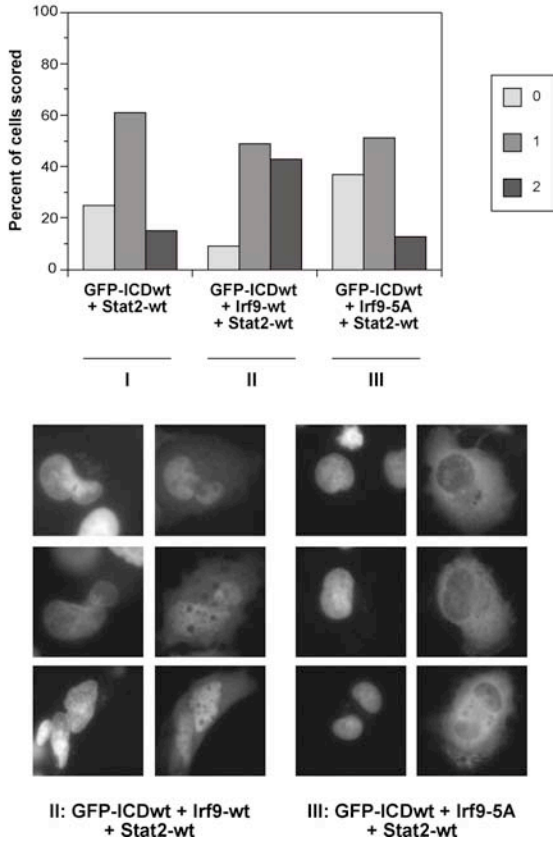

Fig. 6. Mutation of the Irf9 NLS reduces nuclear localization of GFP-ICD. Irf9-deficient U2A cells were transiently transfected with plasmids encoding IFNaR2-ICD fused to GFP (GFP-ICDwt) plus plasmids encoding either Irf9 (Irf9-wt), a version of Irf-9 with mutations in five basic residues of the NLS (Irf9-5A) along with wild type Stat2, as indicated, analogous to Fig. 5A. Similar to Fig. 3, cells were processed, visualized and scored; statistical analysis of the plotted data is shown in the Supplement (Table S5) and representative cells from two of the transfected cultures are shown in the bottom part of the figure.

SUPPLEMENTARY DATA FOR:

El Fiky, Pioli, Azam, Yoo, Nastiuk & Krolewski
Nuclear transit of the intracellular domain of the interferon receptor subunit IFNaR2 requires Stat2 and Irf9

Table S1 Statistical analysis of data in Figure 3

Confidence intervals for nuclear fluorescence intensity scoring

Transfected constructs:	N	% scored = 0 (95% CI)	% scored = 1 (95% CI)	% scored = 2 (95% CI)
I. GFP-ICDwt	54	37 (25-50)	56 (42-68)	7 (2-18)
II. GFP-ICDwt + Stat2-wt	63	29 (19-41)	24 (15-36)	48 (36-60)
III. GFP-ICDm1	47	66 (52-78)	21 (12-35)	13 (6-26)
IV. GFP-ICDm1 + Stat2-wt	17	53 (31-74)	41 (22-64)	6 (0-29)

Mann-Whitney U-test p values

	I. GFP-ICDwt	II. GFP-ICDwt + Stat2-wt	III. GFP-ICDm1	IV. GFP-ICDm1 + Stat2-wt
I. GFP-ICDwt	X	0.002	0.043	0.337
II. GFP-ICDwt + Stat2-wt	0.002	X	0.007	0.007
III. GFP-ICDm1	0.043	0.007	X	0.589
IV. GFP-ICDm1 + Stat2-wt	0.337	0.007	0.589	X

Table S2 Statistical analysis of data in Figure 4

Confidence intervals for nuclear fluorescence intensity scoring

Transfected constructs:	N	% scored = 0 (95% CI)	% scored = 1 (95% CI)	% scored = 2 (95% CI)
I. GFP-ICDwt	50	68 (54-79)	12 (5-24)	20 (11-33)
II. GFP-ICDwt + Stat2-wt	51	45 (32-59)	10 (4-21)	45 (32-59)
III. GFP-ICDwt +Stat2Δ235	50	74 (60-84)	8 (3-19)	18 (10-31)

Mann-Whitney U-test p values

	I. GFP-ICDwt	II. GFP-ICDwt + Stat2-wt	III. GFP-ICDwt + Stat2D235
I. GFP-ICDwt	X	0.023	0.638
II. GFP-ICDwt + Stat2-wt	0.023	X	0.008
III. GFP-ICDwt + Stat2Δ235	0.638	0.008	X

Table S3 Statistical analysis of data in Figure 5A

Confidence intervals for nuclear fluorescence intensity scoring

Transfected constructs:	N	% scored = 0 (95% CI)	% scored = 1 (95% CI)	% scored = 2 (95% CI)
I. GFP-ICDwt	31	45 (29-62)	45 (29-62)	10 (3-26)
II. GFP-ICDwt + Irf9-wt	21	67 (45-83)	19 (7-41)	14 (4-35)
III. GFP-ICDm1 + Irf9-wt + Stat2-wt	25	4 (0-21)	48 (30-67)	48 (30-67)
IV. GFP-ICDm1 + Irf9-wt + Stat2Δ235	19	74 (51-89)	21 (8-44)	5 (0-26)

Mann-Whitney U-test p values

	I. GFP-ICDwt	II. GFP-ICDwt + Irf9-wt	III. GFP-ICDwt + Irf9-wt + Stat2-wt	IV. GFP-ICDwt + Irf9-wt + Stat2 D235
I. GFP-ICDwt	X	0.308	< 0.001	0.099
II. GFP-ICDwt + Irf9-wt	0.308	X	< 0.001	0.638
III. GFP-ICDwt + Irf9-wt + Stat2-wt	< 0.001	< 0.001	X	< 0.001
IV. GFP-ICDwt + Irf9-wt + Stat2 Δ235	0.099	0.638	< 0.001	X

Table S4 Statistical analysis of data in Figure 5B

Confidence intervals for nuclear fluorescence intensity scoring

Transfected constructs:	N	% scored = 0 (95% CI)	% scored = 1 (95% CI)	% scored = 2 (95% CI)
I. GFP-ICDwt	29	76 (58-88)	3 (0-19)	21 (9-39)
II. GFP-ICDwt + Stat2-wt	31	77 (60-89)	13 (5-29)	10 (3-26)

Mann-Whitney U-test p values

	I. GFP-ICDwt	II. GFP-ICDwt + Stat2-wt
I. GFP-ICDwt	X	0.803
II. GFP-ICDwt + Stat2-wt	0.803	X

Table S5 Statistical analysis of data in Figure 6

Confidence intervals for nuclear fluorescence intensity scoring

Transfected constructs:	N	% scored = 0 (95% CI)	% scored = 1 (95% CI)	% scored = 2 (95% CI)
I. GFP-ICDwt + Stat2-wt + vector	69	25 (16-36)	61 (49-72)	15 (8-25)
II. GFP-ICDwt + Stat2-wt + Irf9-wt	70	9 (4-18)	49 (37-60)	43 (32-55)
III. GFP-ICDwt + Stat2-wt + Irf9-5A	71	37 (27-49)	51 (40-63)	13 (7-23)

Mann-Whitney U-test p values

	I. GFP-ICDwt + Stat2-wt + Vector	II. GFP-ICDwt + Stat2-wt + Irf9-wt	III. GFP-ICDwt + Stat2-wt + Irf9-5A
I. GFP-ICDwt + Stat2-wt + vector	X	< 0.001	0.238
II. GFP-ICDwt + Stat2-wt + Irf9-wt	< 0.001	X	< 0.001
III. GFP-ICDwt + Stat2-wt + Irf9-5A	p = 0.238	< 0.001	X

Table S6 Statistical analysis of data from Figure S1

Confidence intervals for cytoplasmic fluorescence intensity scoring

Transfected constructs:	N	% scored = 0 (95% CI)	% scored = 1 (95% CI)	% scored = 2 (95% CI)
GFP-Irf9-wt	49	71 (58-82)	27 (16-40)	2 (0-12)
GFP-Irf9-5A	52	6 (1-17)	72 (58-83)	26 (16-40)

Mann-Whitney U-test p values

	GFP-Irf9-wt	GFP-Irf9-5A
GFP-Irf9-wt	X	< 0.001
GFP-Irf9-5A	< 0.001	X

Confidence intervals for nuclear fluorescence intensity scoring

Transfected constructs:	N	% scored = 0 (95% CI)	% scored = 1 (95% CI)	% scored = 2 (95% CI)
GFP-Irf9-wt	49	0 (0-9)	6 (1-17)	94 (83-99)
GFP-Irf9-5A	51	0 (0-14)	22 (13-35)	80 (67-89)

Mann-Whitney U-test p values

	GFP-Irf9-wt	GFP-Irf9-5A
GFP-Irf9-wt	X	0.184
GFP-Irf9-5A	0.184	X

Figure Legend:

Fig. S1 Mutation of the bipartite Irf9 NLS reduces nuclear accumulation of a GFP-Irf9 fusion protein.

HEK293T cells were transiently transfected with plasmids encoding wild type Irf9 fused to GFP (GFP-Irf9-wt) or a version with mutations in five basic residues of the NLS (GFP-Irf9–5A). Transfected cells were re-plated on fibronectin-coated glass coverslips, fixed and counter-stained with a nuclear dye (Hoechst 33258). Green fluorescent cells were photographed and scored for nuclear and cytoplasmic fluorescence in a random, double-blinded fashion using a scale of 0 (little or no fluorescence), 1 (intermediate fluorescence) or 2 (highest level of fluorescence). A, Percentage of cells scored for nuclear fluorescence at each level of intensity. B, Percentage of cells scored for cytoplasmic fluorescence at each level of intensity. C, Representative cells from each transfected culture are shown below. In each pair of columns, images on the left correspond to blue fluorescence due to nuclear staining, while those on the right correspond to green fluorescence due to GFP protein. Statistical analysis of the plotted data is shown in Table S6.

Figure S1

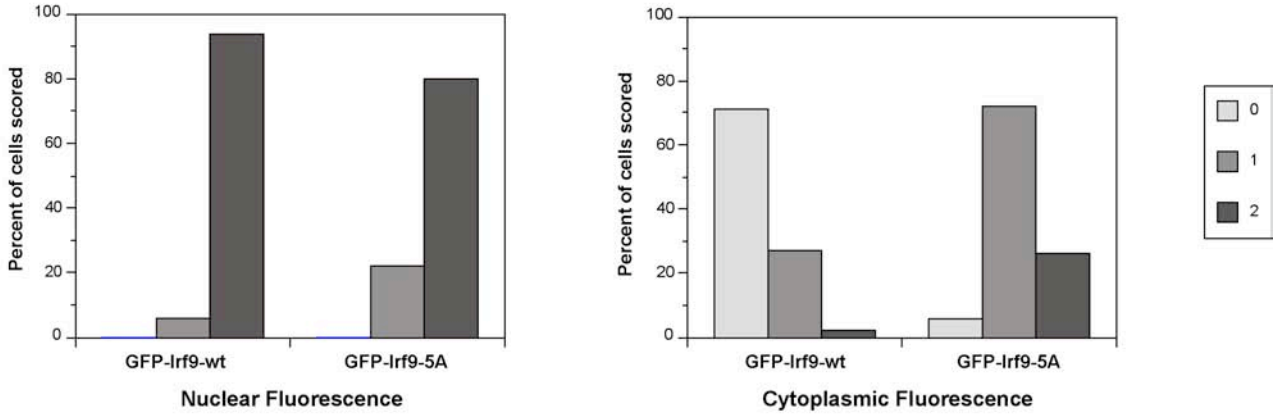
100
80
60
40
20
0
Percent of cells scored
GFP-Irf9-wt
GFP-Irf9-5A
Nuclear Fluorescence
Cytoplasmic Fluorescence
0
1
2

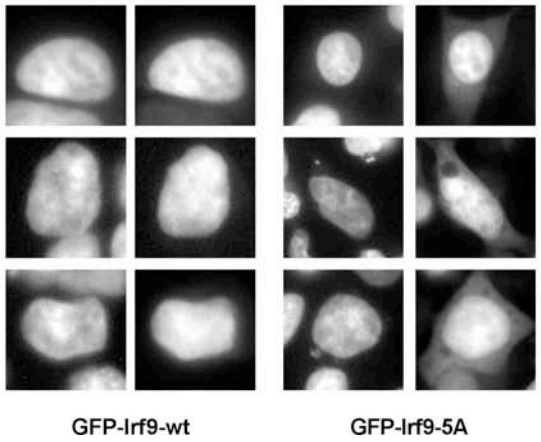
GFP-Irf9-wt
GFP-Irf9-5A